

Formation of Polyphenylene Films on Metal Electrodes by Electrochemical Reduction of Benzenediazonium Salts

Alain Adenier,[†] Catherine Combellas,[‡] Frédéric Kanoufi,[‡] Jean Pinson,[§] and Fetah I. Podvorica^{*,||}

ITODYS, Université Paris 7-Denis Diderot, associé au CNRS (UMR 7086), 1 rue Guy de la Brosse, F-75005, Paris, France, Laboratoire Environnement et Chimie Analytique, CNRS-ESPCI, 10 rue Vauquelin, 75231 Paris Cedex 05, France, Alchimier, Z. I. de la Bonde, 15 rue du Buisson aux Fraises, 91300 Massy, France, and Chemistry Department of Natural Sciences Faculty, University of Prishtina, rr. "Nëna Tereze" nr. 5, Prishtina, Kosovo

Received September 14, 2005. Revised Manuscript Received January 31, 2006

It is possible to form micrometer thick polyphenylene (PP) films by electrochemical reduction of benzenediazonium tetrafluoroborate on metals in acetonitrile. The electrochemical behavior of the PP film is characterized by different electrochemical transient methods and is surprisingly different from that observed with other diazonium salts. The films are analyzed by IR and time-of-flight secondary ion mass spectroscopies; their thickness and conductivity are also characterized. Because they are conductive, these micrometer thick films can be further derivatized by electrochemical reduction of other diazonium salts, for example, nitrophenyl or bromophenyl diazonium salts. Copper can also be deposited on the top of the PP film. The behavior of redox probes on PP films is discussed as well as the origin of this increased conductivity. A simple model for the reaction kinetics of electrografting is presented.

Introduction

It is now well-established^{1–3} that the electrochemical reduction of diazonium salts on carbon,^{4–16} metals,^{17–21} and

silicon^{22–25} leads to the covalent bonding of aryl groups on conductive or semiconductive surfaces—electrografting reaction—as shown in Scheme 1.

More recently, the spontaneous grafting of diazonium salts (i.e., by simple dipping of the substrate in a solution of the diazonium salt) on the same substrates has been observed.^{21,25–28}

The organic layers, which are obtained in this way, are strongly adherent, and the covalent bond between the substrate and the overlayer has been detected by X-ray photoelectron spectroscopy (XPS)²⁰ on metals and by Raman spectroscopy²⁹ and time-of-flight secondary ion mass spectroscopy (ToF-SIMS)³⁰ on carbon. The thickness of these layers can vary from an organized monolayer on Si²⁴ to

* To whom correspondence should be addressed. E-mail: fetahpodvorica@yahoo.com.

[†] Université Paris 7-Denis Diderot.

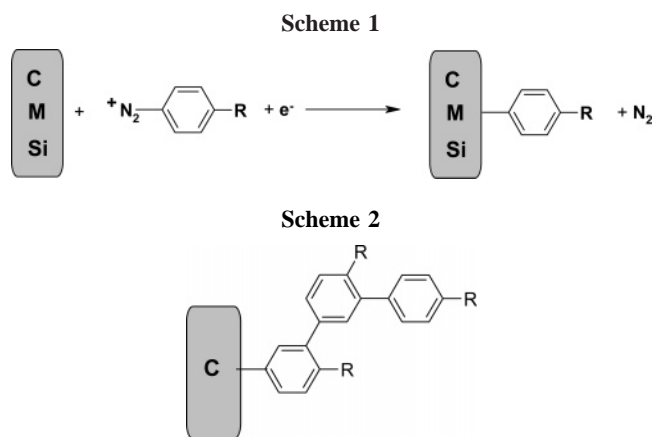
[‡] CNRS-ESPCI.

[§] Alchimier.

^{||} University of Prishtina.

- (1) Pinson, J.; Podvorica, F. *Chem. Soc. Rev.* **2005**, 34, 429.
- (2) Downard, A. J. *Electroanalysis* **2000**, 12, 1085.
- (3) Maeda, H.; Yamauchi, Y.; Ohmori, H. *Curr. Top. Anal. Chem.* **2001**, 2, 121.
- (4) Delamar, M.; Hitmi, R.; Pinson, J.; Savéant, J.-M. *J. Am. Chem. Soc.* **1992**, 114, 5883.
- (5) Allongue, P.; Delamar, M.; Desbat, B.; Fagebaume, O.; Hitmi, R.; Pinson, J.; Savéant, J.-M. *J. Am. Chem. Soc.* **1997**, 119, 201.
- (6) Delamar, M.; Desarmot, G.; Fagebaume, O.; Hitmi, R.; Pinson, J.; Savéant, J.-M. *Carbon* **1997**, 36, 801.
- (7) Bahr, J. L.; Yang, J.; Kosynkin, D. V.; Bronikowski, M. J.; Smalley, R. E.; Tour, J. M. *J. Am. Chem. Soc.* **2001**, 123, 6536.
- (8) Liu, Y. C.; McCreery, R. L. *J. Am. Chem. Soc.* **1995**, 117, 11254.
- (9) Itoh, H.; McCreery, R. J. *Am. Chem. Soc.* **2002**, 12, 10894.
- (10) Anariba, F.; DuVall, S. H.; McCreery, R. L. *Anal. Chem.* **2003**, 75, 4680.
- (11) Ray, K., III; McCreery, R. L. *Anal. Chem.* **1997**, 69, 4680.
- (12) Saby, C.; Ortiz, B.; Champagne, G. Y.; Bélanger, D. *Langmuir* **1997**, 13, 3837.
- (13) Ortiz, B.; Saby, C.; Champagne, G. Y.; Bélanger, D. *J. Electroanal. Chem.* **1998**, 455, 75.
- (14) Kariuki, J. K.; McDermott, M. T. *Langmuir* **1999**, 15, 6534.
- (15) Kariuki, J. K.; McDermott, M. T. *Langmuir* **2001**, 17, 5947.
- (16) (a) Brooksby, P. A.; Downard, A. J. *Langmuir* **2004**, 20, 5038–5045. (b) In aqueous acid solution the azobenzene groups (of polynitro-azobenzene films) as well as most nitro groups were found to be electrochemically inactive, and this was assigned to the inhibition of the conformation changes that accompany the azobenzene redox reaction and to slow ion transport within the compact layer.^{16c} (c) Broobbsky, P. A.; Downard, A. J. *J. Phys. Chem. B* **2005**, 109, 8791.
- (17) Adenier, A.; Bernard, M. C.; Chehimi, M. M.; Cabet-Deliry, E.; Desbat, B.; Fagebaume, O.; Pinson, J.; Podvorica, F. *J. Am. Chem. Soc.* **2001**, 121, 4541.
- (18) Chaussé, A.; Chehimi, M. A.; Karsi, N.; Pinson, J.; Podvorica, F.; Vautrin-UI, C. *Chem. Mater.* **2002**, 14, 392.

- (19) Bernard, M. C.; Chaussé, A.; Cabet-Deliry, E.; Chehimi, M. M.; Pinson, J.; Podvorica, F.; Vautrin-UI, C. *Chem. Mater.* **2003**, 15, 3450.
- (20) Boukema, K.; Chehimi, M. M.; Pinson, J.; Blomfield, C. *Langmuir* **2003**, 19, 6333.
- (21) Adenier, A.; Cabet-Deliry, E.; Chaussé, A.; Griveau, S.; Mercier, F.; Pinson, J.; Vautrin-UI, C. *Chem. Mater.* **2005**, 17, 491.
- (22) Henry de Villeneuve, C.; Pinson, J.; Bernard, M. C.; Allongue, P. *J. Phys. Chem. B* **1997**, 101, 2415.
- (23) Allongue, P.; Henry de Villeneuve, C.; Pinson, J.; Ozanam, F.; Chazalviel, J. N.; Wallart, X. *Electrochim. Acta* **1998**, 43, 2791.
- (24) Allongue, P.; Henry de Villeneuve, C.; Cherouvrier, G.; Cortes, R. *J. Electroanal. Chem.* **2003**, 550, 161.
- (25) Stewart, M. P.; Maya, F.; Kosynkin, D. V.; Dirk, S. M.; Stapelton, J. J.; McGuinness, C. L.; Allara, D. L.; Tour, J. M. *J. Am. Chem. Soc.* **2004**, 126, 370.
- (26) Hurley, B. L.; McCreery, R. L. *J. Electrochem. Soc.* **2004**, 151, B252.
- (27) Combellas, C.; Kanoufi, F.; Pinson, J.; Podvorica, F. *Chem. Mater.* **2005**, 17, 3968.
- (28) Cooke, J. M.; Galloway, C. P.; Bissell, C. E.; Adams, M. C.; Yu, J. A.; Belmont, R.; Amici, M. U.S. Patent 61 109994 A (to Cabot Corp.) and references therein.
- (29) Nowak, A. M.; McCreery, R. L. *Anal. Chem.* **2004**, 76, 1089.
- (30) Combellas, C.; Kanoufi, F.; Pinson, J.; Podvorica, F. *Langmuir* **2005**, 21, 280.



monolayers¹⁰ or thin films, about 2 to 6 nm,^{10,16} on a very flat type of carbon (pyrolyzed photoresist) to fractions of micrometers.³¹ Interestingly, the growth of layers up to 10 nm can also be observed during their spontaneous formation,²¹ and a nonelectrochemical mechanism has been proposed for this reaction.³⁰ A possible model for the structure of the layer has been presented¹⁵ (Scheme 2).

The above electrografting of diazonium salts as well as the anodic electrografting of amines^{32,33} and carboxylates³⁴ are easily characterized by cyclic voltammetry by a peculiar behavior exemplified by the case of 4-nitrobenzenediazonium in Figure 1. In the first scan, a rather broad irreversible peak is observed. It corresponds to the reduction of the diazonium and to the formation of the radical, which binds to the surface. In the second scan, this peaks disappears (or at least becomes very small). Inhibition of the voltammetric response has been assigned to the hydrophobic character of the organic layer, which repels the charged diazonium cation.^{12,13,21} Indeed, using the same 4-nitropolyphenylene (4-NPP) layer, the voltammogram of $\text{Fe}(\text{CN})_6^{4-/3-}$ is so drawn out that it becomes comparable to the background response.

In this paper, we will specify the behavior of benzenediazonium itself on metals. It is quite different from that of other diazonium salts already described. We will show that the organic layer obtained with this salt presents some distinctive conductive and electrochemical properties. These properties will be compared to those of polyphenylene (PP), a polymer, which can be prepared by electrochemical oxidation of benzene, among other methods.³⁵

Experimental Section

All the solvents are reagent grade. The benzenediazonium tetrafluoroborate salt is synthesized as follows.⁴⁴ A total of 0.01

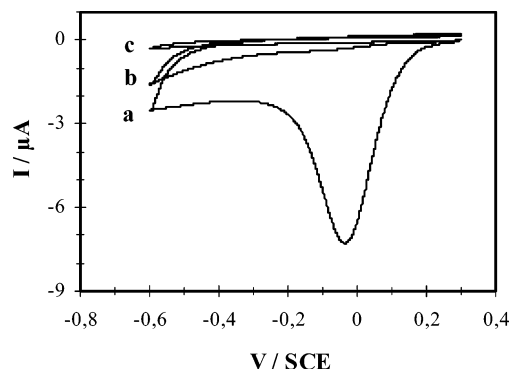


Figure 1. Cyclic voltammetry at a platinum electrode (diameter = 1 mm) in an ACN + 10 mM ${}^+\text{N}_2\text{C}_6\text{H}_4\text{NO}_2\text{BF}_4^-$ + 0.1 M NBu_4BF_4 solution. (a) First and (b) second scans and (c) the same electrode in an ACN + 0.1 M NBu_4BF_4 solution. Scan rate = 0.2 V s^{-1} .

mol of aniline is dissolved in 0.03 mol of HBF_4 . After cooling the solution at $\sim 0^\circ\text{C}$ with ice, a concentrated solution of NaNO_2 (0.015 mol) in water is added. After filtration, the precipitate is washed with a saturated cold solution (10 mL) of NaBF_4 in water and cold ether. The powder is dried and kept in a freezer at -5°C .

The iron, copper, and zinc electrodes are 99.99% purity wires (Goodfellow) embedded in epoxy resin. The copper and iron plates are of 99% purity (Weber métaux, France). They are first polished with a polishing cloth (DP-Nap, Struers, Denmark) using $1 \mu\text{m}$ diamond paste and then with a $0.02 \mu\text{m}$ alumina slurry (Presi, France) in Nanopure water to avoid organic contaminants on the electrodes. They are then rinsed in acetone. All potentials are measured versus the Ag/AgCl or the saturated calomel electrode (SCE) reference.

The solutions with various redox probes are ferrocene (2 mM, NBu_4BF_4 ; 0.1 M, acetonitrile (ACN)), ferricyanide (2 mM, KCl ; 0.1 M, water; pH 7, phosphate buffer), and ruthenium hexamine (2 mM, KCl ; 0.1 M, water; pH 7, phosphate buffer).

The voltammetric experiments are performed with a potentiostat/galvanostat (CH660 A, CH Instruments, U.S.A.).

The best conditions for the formation of a homogeneous film on centimeter electrodes are the following: 100 mL of solution (ACN + 0.1 M NBu_4BF_4 + 10 mM benzenediazonium tetrafluoroborate) in a cylindrical cell, the metal plate electrode centered in the cell, a circular carbon paper counter electrode, and a reference electrode between the metal electrode and the counter electrode. The solution is degassed before the electrolysis, and a flow of nitrogen is maintained in the cell.

Film thicknesses are measured by carving a sharp furrow through the film with either a cutter (on iron) or a sharp tip of hard wood (on copper) and measuring the depth of this furrow with an α Step IQ profilometer from KLA Tencor.

ToF-SIMS spectra are obtained with an ION-TOF IV with Au^+ primary ions at 25 keV; the analyzed zone is $150 \mu\text{m}^2$, and the acquisition time is 75 ms.

- (31) Bureau, C.; Levy, E.; Viel, P. *PCT Int. Appl.*, WO 03018212, 2003.
- (32) Barbier, B.; Pinson, J.; Desarmot, G.; Sanchez, M. *J. Electrochem. Soc.* **1990**, *137*, 1757.
- (33) Adenier, A.; Chehimi, M. M.; Gallardo, I.; Pinson, J.; Villa, N. *Langmuir* **2004**, *20*, 8243.
- (34) Andrieux, C. P.; Gonzalez, F.; Savéant, J.-M. *J. Am. Chem. Soc.* **1997**, *119*, 4292.
- (35) Aeiayach, S.; Lacaze, P. C. *J. Polym. Sci., Part A: Polym. Chem.* **1989**, *27*, 515–526.
- (36) (a) Downard, A. J.; Pletcher, D. *J. Electroanal. Chem.* **1986**, *206*, 147. (b) Hillman, A. R.; Mallen, E. F. *J. Electroanal. Chem.* **1987**, *220*, 351. (c) Grujicic, D.; Pesic, B. *Electrochim. Acta* **2002**, *47*, 2901. (d) D'Alejo, P. C. *J. Electroanal. Chem.* **2004**, *573*, 29.
- (37) Socrates, G. *Infrared Characteristic Group Frequencies*; Wiley: Chichester, U.K., 2001.

- (38) Silverstein, R. M.; Basler, G. C.; Morill, T. C. *Identification Spectrométrique de Composés Organiques*; De Boeck Université: Paris, Bruxelles, 1998.
- (39) Aeiayach, S.; Lacaze, P. C. *J. Polym. Sci., Polym. Chem. Ed.* **1989**, *27*, 515.
- (40) Li, C.; Shi, G.; Liang, Y. *Synth. Met.* **1999**, *104*, 113.
- (41) Combellas, C.; Kanoufi, F.; Mazouzi, D.; Thiébaud, A.; Bertrand, P.; Médard, N. *Polymer* **2003**, *44*, 19.
- (42) (a) Anariba, F.; McCreery, R. L. *J. Phys. Chem. B* **2002**, *106*, 10355. (b) McCreery, R. L.; Dieringer, J.; Solak, A. O.; Snyder, B.; Nowak, A. M.; McGovern, W. R.; DuVall, S. *J. Am. Chem. Soc.* **2004**, *126*, 6200.
- (43) Matnishyan, A. A.; Ambartsumyan, G. V.; Akhnazaryan, T. L. *Hayastani Kim. Handes* **2002**, *55*, 162 (CAN 138:272052).
- (44) Andrieux, C. P.; Pinson, J. *J. Am. Chem. Soc.* **2003**, *125*, 14801.

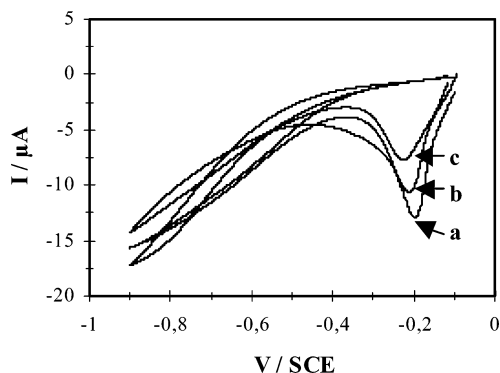


Figure 2. Cyclic voltammety of an iron electrode (diameter = 1 mm) in ACN + 0.1 M NBu₄BF₄ + 10 mM N₂C₆H₅BF₄ solution. (a) 1st, (b) 4th, and (c) 12th scans. Scan rate = 0.2 V s⁻¹.

The IR-attenuated total reflection (ATR) spectra are recorded on a FTIR Bruker Tensor 27 spectrometer equipped with a diamond based ATR sampling platform (Durascope from SensIR Technology). A total of 100 spectra are acquired with 4 cm⁻¹ resolution; the spectra are corrected for CO₂ and H₂O, and the baseline is also corrected.

The scanning electron microscopy (SEM) spectra are obtained with a MEB ZEISS ULTRA II. Two types of images are recorded: secondary ion images to observe the morphology of the surface, and backscattered electron (BSE) images for the observation of the chemical contrast. The images are recorded under 1 and 2 kV voltages and a working distance of 2 mm. The enlargements are varied from 1000 to 50 000.

The ellipsometric measurements are obtained on a Sopra ellipsometer.

The conductivity of the film on copper is obtained by two methods: either (i) making contact to the layer with a piece of carbon paper pressed against the film with a weight of approximately 1 kg or (ii) filling a Pasteur pipet with mercury, lowering the terminal drop until a contact is made with the PP film, and measuring the contact area from a side view taken with a microscope. Comparable results are obtained by the two methods.

Results

Cyclic Voltammety. Figure 2 shows the cyclic voltammograms obtained at an iron electrode immersed in an ACN + 0.1 M NBu₄BF₄ + 10 mM N₂C₆H₅BF₄ solution. The first scan begins at 0.1 V/SCE, that is, the open circuit potential of an iron electrode (the metal is not stable at more positive potentials;¹⁷ Figure 2a); it shows a cathodic peak due to the electrochemical reduction of the diazonium salt, around $E_{pc} = -0.2$ V/SCE. The current decreases slowly with the number of scans (Figure 2b,c after respectively 4 and 12 cycles) without stirring the solution between the cycles. This behavior is quite different from that of 4-nitrobenzenediazonium presented in Figure 1, which is representative of the general behavior of diazonium salts both on carbon and on metals.^{4,17} Similar curves are obtained on copper (Supporting Information, Figure S1) and zinc.

Potentiostatic Measurements. The chronoamperometric response of an iron plate ($s = 8$ cm²) biased at a cathodic potential (-0.8 V/SCE) in an ACN + 10 mM ⁺N₂C₆H₅ BF₄⁻ solution is shown in Figure 3, curve a. Three different regions are observed. Region I shows a decrease of the current from its initial value ($|I| \sim 5$ mA) to a minimum ($|I| \sim 1$ mA) after about 3 s. Region II shows the rise of current from 3

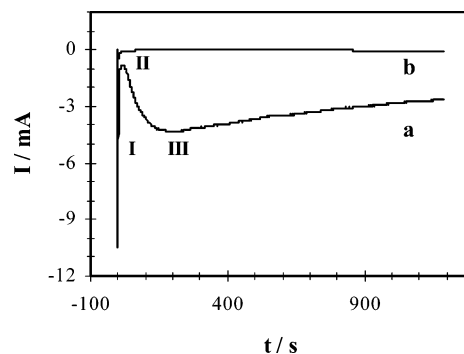


Figure 3. Chronoamperometric curve of an iron plate ($s = 8$ cm²), maintained at $E = -0.8$ V/SCE, in ACN + 0.1 M NBu₄BF₄ + 10 mM (a) N₂C₆H₅BF₄ and (b) N₂C₆H₄NO₂BF₄ solutions.

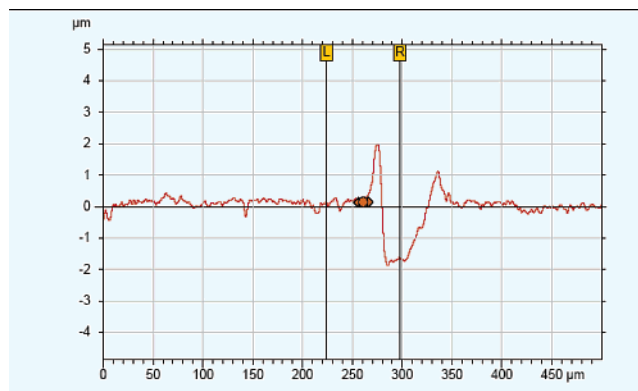


Figure 4. Profilometry of a PP film electrodeposited onto an iron plate. Electrolysis for 20 min at -1.1 V/SCE in an ACN + 0.1 M NBu₄BF₄ + 10 mM ⁺N₂C₆H₅ BF₄⁻ solution.

to about 200 s. Region III corresponds to a slow decrease of the current after 200 s that can be assigned to the ohmic drop in the film. A similar curve is obtained on copper (Supporting Information, Figure S2). In both cases, the shape of the curve is indicative of the formation of a conducting film via a nucleation mechanism.^{35,36} When the iron plate is removed from the solution, a thick, brown film is observed on its surface.

This behavior is very different from that obtained with iron or copper in the presence of other aryldiazonium salts. In the latter case, a very fast decrease of the current is observed as soon as the electrolysis starts. This is assigned to the presence of a film that blocks the electrochemical response of the electrode as shown in Figure 3, curve b. In the latter case, the iron plate is biased at a cathodic potential (-0.8 V/SCE), in an ACN + 10 mM ⁺N₂C₆H₄NO₂BF₄⁻ solution. A similar curve is obtained on copper.

Characterization of the Polyphenylene Layers. *Thickness of the Layers.* A PP layer was prepared on the same iron plate as that used for the potentiostatic measurements ($s = 8$ cm²). It was maintained for 20 min at -1.1 V/SCE in an ACN + 0.1 M NBu₄BF₄ + 10 mM N₂C₆H₅BF₄ solution and thoroughly rinsed in an acetone bath for 10 min. Its thickness was measured by profilometry. With the naked eye, it is seen that the film is homogeneous and its height reaches up to 2 μm (1.7 μm in Figure 4). On a copper electrode that had undergone 10 cycles at 20 mV s⁻¹ between 0 and -2 V/SCE, the thickness of the film was 2.2 μm. This is much thicker than the films obtained with other diazonium salts. For

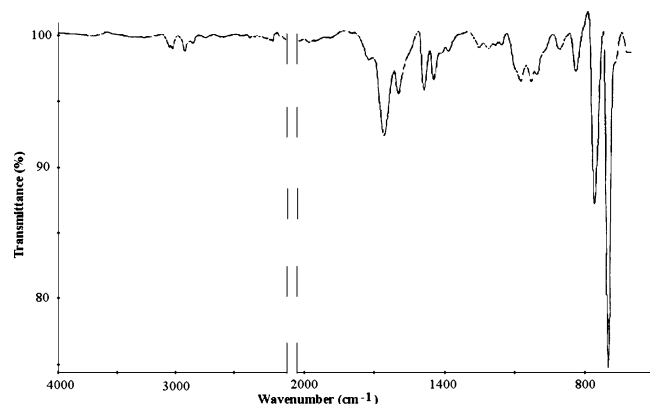


Figure 5. IR spectrum of a PP film on an iron surface.

Table 1. IR Spectrum of a Polyphenyl Film Obtained by Electrodeposition on Iron

bands, cm^{-1}	intensity	assignment ^{37,38}
3060, 3027	w	aromatic C—H stretching vibrations
1733, 1659	m	C—H out-of-plane deformation vibrations
1597, 1487, 1446	m	aromatic C=C stretching vibrations
1075, 1029	m–w	in-plane C—H bending of substituted phenyls
838	m	aromatic C—H out-of-plane vibrations for different substitutions as 1,3-, 1,4-, 1,2,3-, or mono-substituted benzenes
755, 698	s, vs	aromatic C—H out-of-plane vibrations for different substitutions as 1,3-, 1,4-, 1,2,3-, or mono-substituted benzenes

example, layers from 35 to 60 nm thickness were observed by atomic force microscopy (AFM) on Cu, Ni, and Zn modified with 4-dodecylbenzenediazonium tetrafluoroborate ($c = 2 \text{ mM}$, 30 min),¹⁹ and poly(4-nitrophenylene) layers up to 100 nm thickness were obtained on a platinum electrode at very negative potentials.³¹ When observed with an optical microscope, the structure of the film depends very much on the electrolysis conditions (mechanical stirring of the solution, bubbling of nitrogen, geometry of the cell); the best conditions are reported in the experimental part.

IR-ATR Spectroscopy. We have also studied the formation of PP multilayers by IR-ATR spectroscopy. The results are presented in Table 1 and Figure 5. The same iron plate as above was electrografted with a PP layer by a 30 s electrolysis in an ACN + 0.1 M NBu_4BF_4 + 10 mM $+\text{N}_2\text{C}_6\text{H}_5\text{BF}_4^-$ solution at the potential of -1.1 V/SCE , and then the electrode was carefully rinsed in ACN in an ultrasonic bath for 15 min.

First, no significant band could be observed in the $2300\text{--}2130 \text{ cm}^{-1}$ region (stretching of the $\text{N}\equiv\text{N}^+$ bond of the diazonium salt); this confirms the loss of dinitrogen during the electrografting reaction.

The spectrum exhibits two weak bands at 3060 and 3027 cm^{-1} , which correspond to the stretching of aromatic C—H bonds. The medium intensity bands at 1733 and 1659 cm^{-1} are characteristic overtone and combination bands due to C—H out-of-plane deformation vibrations. These bands only appear when phenyl multilayers are present and indicate different substitutions of the benzene ring.^{27,37–39} The bands

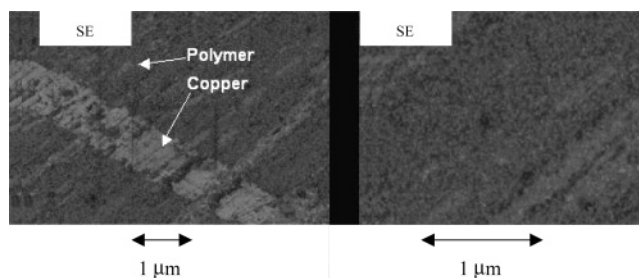


Figure 6. SEM of a PP film on a copper surface. SEs. Left: scratched surface.

Table 2. ToF-SIMS Spectrum of a Polyphenyl Film Obtained by Electrodeposition on Iron^a

m/z	assignment
77	C_6H_5^+
91	$\text{C}_6\text{H}_5\text{CH}_2^+$
105	$\text{C}_6\text{H}_5\text{CH}_2\text{CH}_2^+$
115	$\text{C}_6\text{H}_5\text{CH}=\text{CH}=\text{CH}^+$ or isomer
128	$\text{C}_6\text{H}_5\text{CH}=\text{CH}=\text{CH}=\text{CH}^+$ or isomer
152	$[\text{C}_6\text{H}_5-\text{C}_6\text{H}_5-2\text{H}]^+$
228	$[\text{C}_6\text{H}_5-\text{C}_6\text{H}_4-\text{C}_6\text{H}_5-2\text{H}]^+$
304	$[\text{C}_6\text{H}_5-\text{C}_6\text{H}_4-\text{C}_6\text{H}_4-\text{C}_6\text{H}_5-2\text{H}]^+$

^a Polyphenyl fragments.

at 1597, 1487, and 1446 cm^{-1} correspond to the stretching of C=C bonds in aromatic rings. The bands at 1075 and 1029 cm^{-1} correspond to C—H bending in the plane for substituted phenyls.³⁷ In the $900\text{--}700 \text{ cm}^{-1}$ region one observes the existence of a weak band at 838 cm^{-1} and two strong bands at 755 and 698 cm^{-1} , the latter being stronger than the former. These parts of the spectra indicate the presence of different types of aromatic substitutions such as monosubstitution, 1,3-, 1,4-disubstitution, and 1,2,3-trisubstitution.^{37,40} These different types of substitutions reflect the nonregiospecific attack of the aryl radicals formed during the electrolysis on the different positions of the already attached benzene rings.

ToF-SIMS Analysis. The ToF-SIMS spectrum (Table 2) of a layer obtained on iron in conditions similar to those above confirms its PP character. In addition to the polyphenyl fragments reported in Table 2, the spectrum is dominated by peaks separated by 13 mass units indicating the successive loss of CH groups: 152, 165, 178, 191; 202, 215, 228, 241, 254; 226, 239, 251, 264; and so forth. The same spectrum is obtained when the PP layer is grown on copper.

Scanning Electron Microscopy. A film was prepared on a copper plate electrode (scanned 10 times at 20 mV s^{-1} between -0.2 and -1 V/SCE in an ACN + 0.1 M NBu_4BF_4 + 10 mM $\text{N}_2\text{C}_6\text{H}_5\text{BF}_4$ solution without any stirring of the solution) and rinsed in an acetone bath for 10 min. The film was examined by optical microscopy (Supporting Information, Figures S3 and S4) and SEM (Figure 6). The images obtained with a 1 kV voltage (to decrease the charging effects and observe the outer surface) from the secondary electrons (SEs) and BSEs indicate that the coating is uniform and covered with a rather high rugosity ($0.1 \mu\text{m}$). To observe a clear contrast pertaining to Cu, it is necessary to scratch the film; this indicates that even within the rugosity, the polymer is always present and no pinholes can be observed.

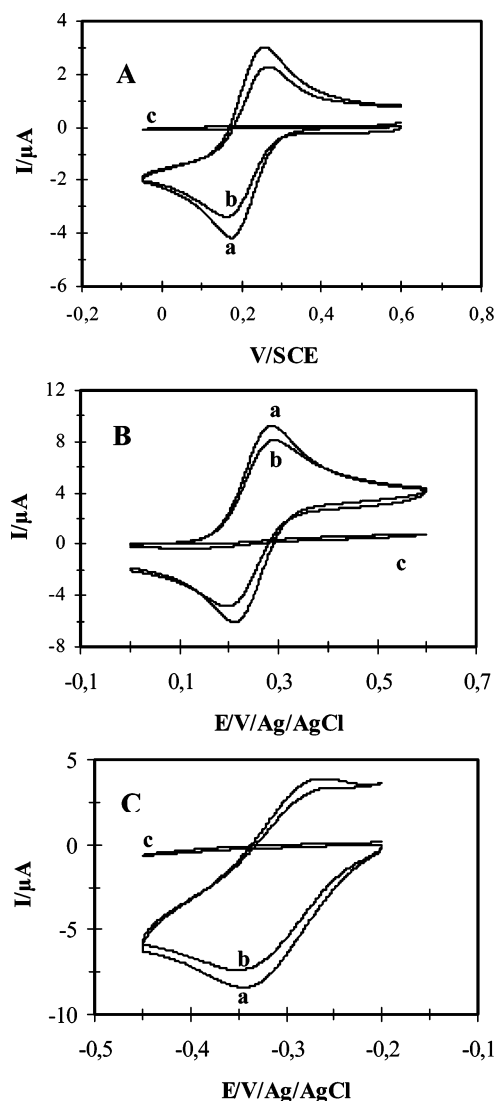


Figure 7. Cyclic Voltammetry of a gold electrode (diameter = 1 mm) in a 0.1 M KCl + (A) 2 mM $\text{K}_3[\text{Fe}(\text{CN})_6]$ aqueous solution, (B) 2 mM ferrocene acetonitrile solution, and (C) 2 mM $[\text{Ru}(\text{NH}_3)_6]\text{Cl}_3$ aqueous solution, pH 7, phosphate buffer. (a) Bare, (b) modified for 25 min in an ACN + 0.1 M NBu_4BF_4 + 10 mM $\text{N}_2\text{C}_6\text{H}_5\text{BF}_4$ solution, and (c) modified for 25 min in an ACN + 0.1 M NBu_4BF_4 + 10 mM $\text{N}_2\text{C}_6\text{H}_4\text{NO}_2\text{BF}_4$ solution. Scan rate = 0.2 V s^{-1} .

Film Conductivity. The resistance of the film was measured on the sample used for recording SEM images. It was obtained by contacting the PP layer with a carbon paper or with a mercury drop at the end of a capillary (see Experimental Section); both methods gave comparable results. After measuring the conductivity, the thickness of the film was obtained both by ellipsometry (45 nm as the average of two measurements) and by profilometry (52 nm as the average of 10 measurements). From the resistance of the PP sheet and its thickness, it was possible to obtain the conductivity of the PP film ($2.5 \pm 0.5 \times 10^{-6} \text{ S cm}^{-1}$).

Cyclic Voltammetry of Redox Probes. We have examined the behavior of the $\text{Fe}(\text{CN})_6^{4-/3-}$ couple (Figure 7A), an often investigated redox probe, on substituted PP layers. Although the reversible voltammogram of this couple is completely inhibited on a 4-NPP layer,²¹ one can observe little difference between its voltammogram on a bare gold electrode and the same electrode derivatized with a thick PP film. A gold electrode was used for this analysis because the redox

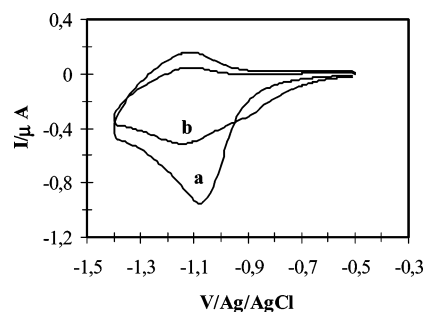


Figure 8. Voltammograms of a gold electrode (diameter = 3 mm) electrografted in ACN + 0.1 M NBu_4BF_4 (a) with 4-nitrophenyl groups and (b) successively with phenyl and 4-nitrophenyl groups. Scan rate = 0.2 V s^{-1} .

potential of $\text{Fe}(\text{CN})_6^{3-/4-}$ is more positive than the oxidation potential of iron. The same behavior was observed with ferrocene (Figure 7B) on a gold electrode modified with a PP film. Similar measurements were achieved with gold and copper electrodes modified with PP film in the presence of $[\text{Ru}(\text{NH}_3)_6]^{3+/2+}$ in an aqueous solution. The voltammograms obtained also show little difference between a bare gold and copper electrodes and the same electrodes derivatized with a thick PP film (Figure 7C for Au and Supporting Information, Figure S5 for Cu).

Further Derivatization of the PP Film with Nitrophenyl and Bromophenyl Groups and with Copper. Because the PP layer obtained by reduction of benzenediazonium ions is fairly conductive, it should be possible to use this organic conducting layer as an electrode to further derivatize the surface by reduction of a different diazonium salt as was already achieved on 4-NPP films.^{16b,31} Following the formation of the PP film on the iron electrode, the electrode was rinsed as usual, immersed into a solution of ACN + 5 mM $^+\text{N}_2\text{C}_6\text{H}_4\text{NO}_2 \text{BF}_4^-$ + 0.1 M NBu_4BF_4 and electrografted for 10 min at -0.8 V/Ag/AgCl , to derivatize the PP film with nitrophenyl groups. The voltammogram of this electrode, reported in Figure 8, curve b, shows a reversible wave at $E_{\text{pc}} \sim -1.1 \text{ V/Ag/AgCl}$, which is characteristic of the reduction of the nitrophenyl groups. A difference in the wave intensity and, therefore, in the surface concentration of the nitrophenyl groups is observed when comparing this wave with those obtained when nitrophenyl groups are directly grafted on gold. This indicates a lower concentration on the surface of the PP film.

We have also electrografted an iron plate covered with a PP film with bromophenyl groups (through the reduction of 4-bromobenzenediazonium), and we have observed the PP + BrPP film by ToF-SIMS measurements in the static mode. The spectrum shows the presence of a doublet at $m/z = 79$, 81 (Br^-), a triplet at $m/z = 158$, 160, 162 (Br_2^-), and fragments at $m/z = 118$, 120 ($\text{C}_3\text{H}_4\text{Br}^-$) and $m/z = 295$, 297 ($\text{C}_{17}\text{H}_{12}\text{Br}^-$) with intensities compatible with the isotopic abundance of bromine. In addition, fragments corresponding to C_6H_5^+ and $\text{C}_6\text{H}_5\text{CH}_2\text{CH}_2^+$ were observed. These data clearly indicate the formation of a 4-bromophenylene layer on the top of the PP film.⁴¹

The iron electrode electrografted with a PP film was used as a cathode for the electrolysis of a 20 mM CuSO_4 solution in ACN, and the characteristic bright color of a homogeneous

copper film could be observed on the top of the PP film. This provides a simple method for the fabrication of a molecular junction such as that investigated by McCreery et al., which presents conductance switching.⁴²

Discussion

Obtention of the PP Film. Cyclic voltammetry and potentiostatic curves obtained during the reduction of benzenediazonium are strikingly different from those observed with all other diazonium salts and specifically with 4-nitrobenzenediazonium where a number of electrochemical data have been reported on different electrodes. For all previously studied diazonium salts, the reduction of the diazonium cation is severely inhibited in the second scan, while in the case of benzenediazonium investigated here, a slow decrease of the peak current is observed with the number of scans. This implies the formation of a conductive film.⁴³ It should be noted that this behavior is dependent on the substrate on which the film is grown. On carbon, at concentrations lower than 1 mM, the wave keeps a nearly constant height in the second scan⁴⁴ and there is little blocking of the electrode. At concentrations from 1 mM to 10 mM, the PP films are not as thick as those observed on iron. Because the conductivity of the PP film is higher than that of substituted PP films, it is possible to grow micrometer thick PP films on conductors such as Fe, Cu, or Zn. On low conductivity metals such as TiN or thin TaN/Ta (Ta deposited by physical vapor deposition) that are used in the microelectronic industry, the films that can be obtained under similar conditions are much thinner (we measured 0.42 μm for TiN and 0.33 μm for TaN/Ta under conditions where 2 μm films are obtained on iron). On different metals, these films are strongly adherent to the surface as they resist ultrasonic rinsing and are likely covalently bonded to iron as in the case of the diazonium salt of 4-aminocarboxylic acid for which the covalent bond has been observed by XPS.²⁰ The conductivity of the film will be discussed further.

Structure of the PP Film. The ToF-SIMS spectra evidence the presence of fragments corresponding to biphenyl, terphenyl, and quaterphenyl and the degradation of the layer by stepwise loss of CH fragments. This is in agreement with the PP structure of the layer. To determine how the phenyl rings are attached to each other, we can compare our results to those obtained with the thoroughly investigated poly(*p*-phenylene) (PPP) polymer.⁴⁵ This polymer^{46,47} can be prepared by a number of chemical^{48–50} or electrochemical⁴⁵ ways. In the latter case, films of variable thicknesses can be obtained.^{35,51,52}

There is a very important difference between the films described in this paper and the PPP films mentioned above, as the latter are only physically adsorbed on the metal surfaces. Therefore, the PPP films obtained on polished iron surfaces (by electrochemical polymerization of benzene in concentrated sulfuric acid in the presence of an anhydrous Lewis acid) are easily peeled off the electrode surface because of the poor attachment of the film on the metal.⁵³

Under proper electrochemical conditions (0.1 M benzene + 0.1 M NBu_4BF_4 in SO_2 at -20°C) it is possible to grow nearly perfect PPP films where all the rings are para substituted.^{39,45,54} Lacaze⁴⁵ et al. have shown that the IR spectrum of PPP with a strictly linear structure should not have absorption bands in the 850–900 cm^{-1} and 1590–1600 cm^{-1} regions. Adsorption at 800 cm^{-1} should be very strong, and for high molecular weight material, this band should be the only one detectable in the 900–600 cm^{-1} range (see, for example, Figure 6.6 of ref 38). As can be observed on the spectrum (Table 1, Figure 5), this is far from being the case for the PP film obtained by reduction of benzenediazonium. The IR-ATR spectrum is indicative of a rather disordered film with several types of substitution, and in addition, it is not possible to exclude cross-linking between the chains.

Mechanism for PP Film Formation. The mechanism leading to the spontaneous (nonelectrochemical) formation of a film has been discussed previously.³⁰ The same type of mechanism should take place when the PP film has been produced electrochemically, and we will limit our comments to the points specific to the electrochemical formation of the PP film. Two significant differences appear by comparison with the nonelectrochemical mechanism applied to substituted diazonium salts, which has been discussed previously: (i) the reduction of the diazonium salts by an electron transfer through the film should be possible at the surface of this film as a result of the increased film conductivity. For the same reason the reoxidation of the intermediate cyclohexadienyl radical should be possible at the surface of the film by transfer of an electron to the electrode (Scheme 3), and (ii) three positions, including the para position, should be available for the substitution of the already attached phenyl ring (if one excludes for steric reasons the positions ortho to the former aryl–aryl bond).

Let us now consider the initial formation of the film. The potentiostatic curve shown in Figure 3 indicates that in region II where the current increases, the formation of the film proceeds by a nucleation mechanism⁴⁵ where small nuclei are formed on the surface separated one from the other. Such nuclei have already been observed by AFM during the initial stages of the grafting of diazonium salts on carbon^{14,15} and metals.^{19,21}

This nucleation mechanism implies that the attack of a phenyl radical is faster on an already grafted phenyl group (k_{nucleus}) than on the metallic surface (k_{metal}) as sketched on

(45) Lacaze, P. C.; Aeiyaich, S.; Lacroix, J. C. *Handbook of Organic Conductive Molecules and Polymers: Synthesis and Electrical Properties*; John Wiley & Sons, Ltd.: New York, 1997; Vol. 2, pp 205–270.

(46) Gram, G.; Leditzky, G.; Ullrich, B.; Leising, G. *Adv. Mater.* **1992**, 4, 36.

(47) Lee, C. H.; Kang, G. W.; Jeon, J. W.; Song, W. J.; Seoul, C. *Thin Solid Films* **2000**, 363, 306.

(48) Kovacic, P.; Jones, M. B. *Chem. Rev.* **1987**, 87, 357.

(49) Yamamoto, T.; Hayashi, Y.; Yamamoto, A. *Bull. Chem. Soc. Jpn.* **1978**, 51, 2091.

(50) VanKerckhoven, H. F.; Gilliams, Y. K.; Stille, J. K. *Macromolecules* **1972**, 5, 541.

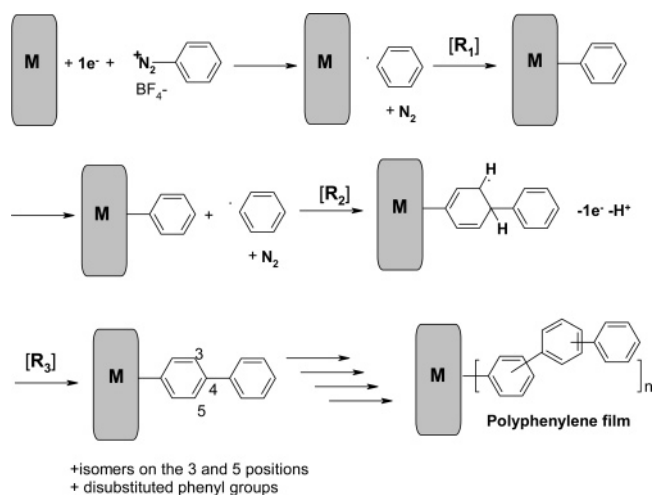
(51) Kvarnström, C.; Ivaska, A. *Synth. Met.* **1991**, 41–43, 2917.

(52) Pham, M.-C.; Aeiyaich, S.; Moslih, J.; Soubiran, P.; Lacaze, P. C. *J. Electroanal. Chem.* **1990**, 277, 327.

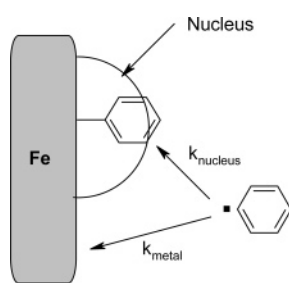
(53) Ye, J. H.; Chen, Y. Z.; Tian, Z. W. *J. Electroanal. Chem.* **1987**, 229, 215.

(54) Aeiyaich, S.; Lacaze, P. C.; Dubois, J. E. *J. Chem. Soc., Chem. Commun.* **1986**, 1668.

Scheme 3



Scheme 4



Scheme 4. This can be compared with recent results from Bélanger et al.⁵⁵ who recorded (with an electrochemical quartz microbalance) the mass of the 4-NPP film deposited on a gold electrode as a function of the potential. During the first negative scan of the voltammogram he observed two approximately straight lines: the first one obviously corresponds to the grafting of the 4-nitrophenyl radicals on the metal, and the second one corresponds to the grafting on the first formed organic layer. The slope of the second line is slightly lower than that of the first one, indicating that the attack of a 4-nitrophenyl radical on 4-nitrophenylene is slightly slower than on gold contrary to what we observe with phenyl radicals on iron.

An estimate of the rate of attack of the phenyl radical on the PP nucleus, k_{nucleus} , can be obtained by using the surface concentration of the phenyl group ($\Gamma \sim 13 \times 10^{-10} \text{ mol cm}^{-2}$)⁵⁵ and assuming that the reaction between the phenyl radical and immobilized phenyl groups has the same rate constant as that of a phenyl radical with benzene in solution, k_{sol} ($k_{\text{sol}} = 10.3 \times 10^5 \text{ mol}^{-1} \text{ L s}^{-1}$),⁵⁶ hence, $k_{\text{nucleus}} \sim k_{\text{sol}}\Gamma \sim 1.3 \text{ cm s}^{-1}$.

Another possibility is to compare solution kinetics to surface reaction kinetics. Owing to the value of k , one can propose that the activation free energy for the solution reaction is mainly the standard activation free energy, $\Delta G_{\text{sol}}^{0\ddagger}$. Then the activation energy for the surface reaction is estimated using the relation derived from the Marcus model between electrochemical (surface reaction) and solution

standard activation energies: $\Delta G_{\text{sol}}^{0\ddagger} = 2\Delta G_{\text{surf}}^{0\ddagger}$. One then obtains $k_{\text{nucleus}} = Z_{\text{nucleus}}(k_{\text{sol}}/Z_{\text{sol}})^{1/2}$, where Z_{nucleus} and Z_{sol} are respectively the heterogeneous and bimolecular (solution) collision frequencies, $Z_{\text{sol}} = 3 \times 10^{11} \text{ mol}^{-1} \text{ L s}^{-1}$ and $Z_{\text{nucleus}} = (RT/2\pi M)^{1/2} \sim 5 \times 10^3 \text{ cm s}^{-1}$. This leads to $k_{\text{nucleus}} \sim 8 \text{ cm s}^{-1}$. Although the two values found for k_{nucleus} are somewhat different, they are of the same order of magnitude, which is not unexpected in view of the rather simple model.

One can then compare those theoretical values to experimentally available data. An apparent value of the surface reaction rate can be obtained from the evolution of the film thickness under potentiostatic conditions and then (see Figure 3) approximately constant current conditions:

$$k_{\text{nucleus,app}}[\text{C}_6\text{H}_5^\bullet]_{\text{nucleus}} = \rho/M \text{ dl/dt}$$

where ρ is the density of the PP film (estimated $\rho \sim 1.2 \text{ g cm}^{-3}$), M is the molecular mass of the monomeric fragment of the PP film ($M = 76$), l is the film thickness, and $[\text{C}_6\text{H}_5^\bullet]_{\text{nucleus}}$ is the concentration of the phenyl radical in the solution at the film surface. Because most of the radicals are formed upon diazonium reduction, this consumption of $\text{C}_6\text{H}_5^\bullet$ in the nucleation process may be related to the current required for the radical formation by diazonium reduction, $i_{\text{nucleation}}$, by

$$i_{\text{nucleation}}/FA = k_{\text{nucleus,app}}[\text{C}_6\text{H}_5^\bullet]_{\text{nucleus}}$$

with A being the electrode surface area ($A = 8 \text{ cm}^2$).

If a linear variation of the film thickness, l , is assumed with the electrolysis time (a film of $1.72 \mu\text{m}$ is obtained within 10 min), one obtains $i_{\text{nucleation}} \sim 3 \text{ mA}$ for an 8 cm^2 electrode. This value is in rough agreement with Figure 3 and shows that the Faradaic efficiency of the film growth is close to 100%. This result does not fit that obtained with 4-nitrobenzenediazonium by Bélanger et al.⁵⁵ who observed with gold and 4-nitrobenzenediazonium a much lower efficiency and, therefore, much thinner films. This also indicates that, in our case, most of the electrode current is used for the one-electron reduction of the diazonium and that the reduction of the phenyl radical at the PP film is negligible. Moreover, a value of $k_{\text{nucleus,app}}$ might be obtained from $i_{\text{nucleus}}:k_{\text{nucleus,app}} (\text{cm s}^{-1}) \sim 4 \times 10^{-3}/[\text{C}_6\text{H}_5^\bullet]_{\text{nucleus}}$ with $[\text{C}_6\text{H}_5^\bullet]_{\text{nucleus}}$ in mM. Therefore, two different conclusions may be obtained from those calculations: either (i) the concentration of the phenyl radical at the film surface, $[\text{C}_6\text{H}_5^\bullet]_{\text{nucleus}}$, equals the diazonium bulk concentration (10 mM) and the surface rate reaction is $k_{\text{nucleus,app}} \sim 4 \times 10^{-4} \text{ cm s}^{-1}$, which is much slower than what could be expected from the above theory, or (ii) the theoretical order of magnitude is correct, and $[\text{C}_6\text{H}_5^\bullet]_{\text{nucleus}}$ is much lower than the diazonium bulk concentration and is of the order of 10^{-6} M . The first proposal seems doubtful because it is unlikely that the concentration of the phenyl radical at the film surface is 10 mM; the latter proposal is conceivable if one remembers that the phenyl radical could also undergo H-atom abstraction from the solvent⁴⁴ and reduction (Scheme 4).

Film Conductivity. The film conductivity measured above for a PP film grown on a copper electrode ($\sigma_{\text{PP}} = 2.5 \times$

(55) Laforgue, A.; Addou, T.; Bélanger, D. *Langmuir* **2005**, *21*, 6855.

(56) Kryger, R. G.; Lorand, J. P.; Neal, R.; Herron, N. R. *J. Am. Chem. Soc.* **1977**, *99*, 7589.

$10^{-6} \text{ S cm}^{-1}$) can be compared with that of the molecular junctions obtained by McCreery et al.^{42b} These junctions were made by growing polyphenyl, biphenyl, terphenyl, or 4-nitroazobenzene films (by reduction of the corresponding diazonium salt) on an especially flat type of carbon (Pyrolized Photoresist Film) and making contact at the other extremity by a Hg drop or a Ti film. The thickness of these layers was perfectly controlled, and the resistance of the junctions could be measured. They obtained the following values between carbon and mercury: $\sigma_{\text{C}_6\text{H}_5} = 2.45 \times 10^{-7} \text{ S cm}^{-1}$ for a phenyl monolayer, $\sigma_{\text{C}_{12}\text{H}_{10}} = 1.03 \times 10^{-9} \text{ S cm}^{-1}$ for a biphenyl monolayer, and $\sigma_{\text{C}_{18}\text{H}_{14}} = 4.10 \times 10^{-10} \text{ S cm}^{-1}$ for a terphenyl monolayer. Between carbon and Ti the resistance of a 4-nitroazobenzene layer varied, on one example, from 38 k Ω soon after the fabrication to 249 M Ω after 6 days. This increased resistance is related to an initial reduction of the nitro groups during the deposition of Ti and further slow reoxidation by air. These values correspond to a conductivity varying from $\sigma_{\text{NAB}} = 4.7 \times 10^{-9} \text{ S cm}^{-1}$ to $\sigma_{\text{NAB}} = 7.6 \times 10^{-11} \text{ S cm}^{-1}$. Although the data of McCreery et al.^{42b} and those of the present paper are obtained on different materials, our value of $\sigma_{\text{PP}} = 2.5 \times 10^{-6} \text{ S cm}^{-1}$ and that of a phenyl monolayer $\sigma_{\text{C}_6\text{H}_5} = 2.45 \times 10^{-7} \text{ S cm}^{-1}$ are not too different. But our value for the resistance of a PP film is much lower than that of a biphenyl or terphenyl layer. The conductivity of the poly(4-nitroazobenzene) film is at least 2 orders of magnitude lower than that of the PP film indicating that PP films are much better conductors than other substituted PP films.

The resistance of PPP films has been measured:⁴² $\sigma_{\text{dc}} \sim 10^{-8} \text{ S cm}^{-1}$ in the undoped state, $\sigma_{\text{dc}} \sim 50 \text{ S cm}^{-1}$ when doped with K^+ , and even 500 S cm^{-1} when doped with AsF_6^- . Our films appear, as could be expected, closer to undoped PPP films. Moreover, we have used IR spectroscopy to confirm the absence of doping by NBu_4^+ . Careful comparison of the film IR spectrum with that of NBu_4^+ allowed this possibility of doping to be ruled out (the small aliphatic bands of the spectrum in Figure 5 do not correspond to NBu_4^+ but to contamination).

The origin of the increased conductivity of the PP film can be discussed in view of the results obtained with films derived from 4-substituted diazoniums. The main difference is the absence of any substituent on the 4 position. McCreery has assigned the high conductivity state of molecular junctions obtained with azobenzene, bi- or terphenyl, to the existence of planar, conjugated quinoid forms.⁴² Such structures would be possible, at least in a transient fashion, with PP films but not with 4-substituted PP films. Another possibility would be that the film is porous with nanometer sized pinholes (the SEM images exclude larger pinholes).

The conductivity mechanism of monolayers of phenyl, bi, and terphenyl has been investigated by Anariba and McCreery.^{42a} On the basis of the temperature dependence of the current, they proposed a temperature-dependent tunneling mechanism for phenyl and biphenyl layers and also for terphenyl layers below 5 °C. For longer molecules as in our case, the conductivity should be temperature-dependent but should decrease with the thickness of the layer (d) either as $\exp(-cd)$ or as d^{-1} ; this is clearly not what we observe

by comparing the values of Anariba and McCreery for a monolayer to ours for micrometer layers. Obviously more data should be obtained on thick PP films to be able to reach a conclusion.

Redox Probes. The response of redox probes on PP films (Figure 7) is also very different from that of substituted PP films such as 4-NPP. Whatever the probe, either negatively as $\text{Fe}(\text{CN})_6^{4-/3-}$ or positively charged as $\text{Ru}(\text{NH}_3)_6^{3+/2+}$ or Fc^+/Fc , in aqueous or aprotic medium, there is little difference between a bare electrode and an electrode modified by a micrometer thick layer of PP film. On a glassy carbon electrode modified by simple dipping²¹ in a solution of 4-nitrobenzenediazonium (10 mM ACN, 1 h) or by electrografting of the same salt (5 mM ACN, $E = -0.7 \text{ V/SCE}$, 240 s) or under the conditions of Figure 7,¹² the response of $\text{Fe}(\text{CN})_6^{4-/3-}$ is completely inhibited in an aqueous medium. The same result is obtained with $\text{Ru}(\text{NH}_3)_6^{3+/2+}$ on a carbon electrode¹² and on gold (Figure 7C) and copper. The response of the quinone/hydroquinone couple is also significantly affected on the same surface.¹² The reasons for this blocking behavior of the 4-nitro and 4-carboxypolyphenylene layers have been thoroughly discussed by Bélanger et al.¹² To summarize, in an aqueous medium, the blocking effect was assigned to hydrophilic/hydrophobic interactions preventing the redox probe from reaching the electrode. The behavior of $\text{Ru}(\text{NH}_3)_6^{3+/2+}$ is particularly demonstrative; its response is completely blocked by a 4-NPP layer but unaffected by a 4-carboxyphenylene (4-CPP) layer. In the same way, $\text{Fe}(\text{CN})_6^{4-/3-}$ ions are blocked by a deprotonated 4-CPP layer but not by the same protonated layer; this is clearly an effect of electrostatic repulsion in the PP layer. In an aprotic medium (ACN), the blocking effect observed both with hydrophilic ($\text{Fe}(\text{CN})_6^{4-/3-}$) and with hydrophobic (ferrocene) probes was assigned to the existence of a compact layer preventing both probes from reaching the electrode. The compactness of the layers obtained by reduction of diazonium salts has been recently supported by Downard.^{16b}

The PP films examined in this paper must be even more hydrophobic, are much thicker than the 4-NPP layers examined by Bélanger et al., and, therefore, must also prevent the different hydrophilic redox probes from reaching the electrode. It must be concluded that the electron transfer to these probes must take place at the surface of the film, which is conductive enough to act as an electrode. The same reason must explain why the response of the diazonium ion is not inhibited. An alternative possibility would be that the film is porous enough to allow the molecules to reach the electrodes. But in this case, the pinholes should be nanometer sized because they cannot be observed on the SEM images with 10–100 nm resolution (cf. Figure 5).

Conclusion

The PP films that are obtained on metals such as iron, copper, or zinc behave differently from their substituted analogues. They do not show the blocking of the electrode generally observed with substituted PP films. This is related to their higher conductivity that permits overlayers of

substituted PP films on copper to be grown. This increased conductivity is related to the different structure of the film, where the substitution pattern is different (three positions, including the para position, being available on each phenyl ring for further substitution). The kinetics of the grafting reaction has been estimated: the rate of reaction of the phenyl radical on the PP layer is on the $1\text{--}10\text{ cm s}^{-1}$ range.

Acknowledgment. We are grateful to Sylvie Verneyre and Géraldine Hallais (Alchimie) for their help with the ToF-SIMS, profilometric, and ellipsometric experiments.

Supporting Information Available: Cyclic voltammetry, chronoamperometric curve, and optical and scanning electron microscopy images of copper electrodes (PDF). This material is available free of charge via the Internet at <http://pubs.acs.org>.

CM052065C